An Adaptive Marked Point Process Filtering Approach for Decoding Cognitive Performance

Saman Khazaei, Student Member, IEEE, and Rose T. Faghih, Senior Member, IEEE.

Abstract—The cognitive performance state is a hidden brain state that can be decoded from behavioral data. One of the challenges in the performance decoder design realm is specifying an informative model and decoder that can realistically reflect the performance dynamics. We employ an autoregressive conditional heteroskedasticity (ARCH) models to capture performance volatility over time and represent a performance state that evolves through a nonlinear and timevarying model. Leveraging a marked point process (MPP) framework, we decode the performance state from a sequence of correct/incorrect responses and reaction times via a Bayesian state-space approach within particle filtering. The MPP framework enables us to account for the reaction times associated with correct responses. We use both experimental and simulated data to evaluate the proposed performance decoder. Findings from experimental data reveal a reliable state estimation outcome that may preserve the environmental impact. Our simulation study depicts the reliability of the decoder. The designed decoder provides an adaptive framework to preserve the information within the process noise and decode the hidden performance state from behavioral data. The proposed performance decoder has potential applications in human-machine interaction, smart workplaces, and future educational settings.

I. Introduction

The term cognitive performance state refers to a dynamic and hidden brain state that indicates an overall performance of human cognitive function [1]. Tracking the trajectory of the hidden performance state requires a decoder that decodes the state from the available observation. While various decoder design procedures can be employed to estimate the underlying performance state, an ideal decoder is supposed to reveal the dynamic of the performance state in a realistic way. In a real-world scenario, external factors, such as music, can affect performance over time [2]. Hence, a model must account for such volatility that can increase or decrease in response to various environmental conditions. On the other hand, specifying a set of informative observations would be another crucial step in designing a performance decoder. Inspired by the autoregressive conditional heteroskedasticity (ARCH) model jointly with the marked point process (MPP) framework [3]–[8], we account for the volatile behavior of performance state and decode the performance state from

This work was supported in part by NSF CAREER: MINDWATCH: Multimodal Intelligent Noninvasive brain state Decoder for Wearable AdapTive Closed-loop arcHitectures under Grant 2226123 and in part by the New York University (NYU) start-up funds.

S. Khazaei and R. T. Faghih are with the Department of Biomedical Engineering, New York University, New York, NY 10010 USA. Corresponding author: Rose T. Faghih (e-mail: rfaghih@nyu.edu). Rose T. Faghih served as the senior author.

behavioral data collected during the n-back task. The nback task is a type of cognitive task that requires working memory usage [2], [9]. Working memory is a basic cognitive function that enables the temporary holding and manipulation of data [9]–[11]. While working memory is a basic cognitive function, it has a pivotal role in higher cognitive function and engages in several cognitive tasks [12]. In this research, we investigate the n-back task as a working memory task of interest. Several studies present a potential impact of music type on the cognitive performance state [1], [2]. In this research, to mimic the potential impact of external stimuli on performance, we consider the music as a form of external auditory stimulation, and the studied n-back task has been performed under 4 different conditions: no background music, relaxing background music, exciting background music, and deep learning-generated relaxing music [1], [2].

The Bayesian state-space approach is one of the common approaches to model and decode the performance state. It was developed mainly based on Bayesian principles and can offer a label-free estimation paradigm [7], [8], [10], [13]–[17]. Specifically, if utilized with the expectationmaximization (EM) framework, the performance state trajectory and its dynamics can be decoded from the available sequential observations and independent of any training sessions. Linear models with time-invariant process noise variance are commonly used within state-space representations [18]–[23]. However, incorporating an adaptive innovation term with time-varying variance within the performance state model can resemble real-world settings where external factors influence the performance state [7], [8]. The ARCH framework is widely used in modeling the financial time series, and it enables state models to reflect the degree of variation over a period of time [24], [25]. Cognitive performance can be affected by multiple external factors such as music [2]. To be able to account for the surrounding effects within the dynamics of the state, we model the process noise via the ARCH framework, and we use the autoregressive-ARCH (AR-ARCH) model to represent the hidden performance state [7], [8].

Once the state model is specified, a performance state can be decoded from the available set of observations such as a sequence of correct/incorrect responses and reaction times (i.e., response times) [26]–[30]. Previously, decoders have been employed to decode the performance state from the sequence of responses coupled with the reaction times [1], [9]; the autoregressive (AR) and AR-ARCH models have been considered for modeling the hidden performance state, and the corresponding decoders have utilized the pairs of

binary and continuous (BiCo) observations to estimate the trajectory of performance [1], [7]–[9]. While the pairs of correct/incorrect responses and reaction times are informative indices of performance, utilizing this type of observation can potentially lead to the overestimation of performance where an incorrect response is accompanied by a fast reaction time. To address this concern, the MPP framework can be employed, and the hidden performance can be decoded from the sequence of responses (point process) as well as the reaction time (marks) associated with successful trials. The MPP framework is commonly applied in neuroscience to link the ensemble neural spiking activity (point process) to the relevant covariates [4]–[6], [8].

In this research, we propose the MPP-ARCH based performance decoder that can track the underlying performance trajectory from the correct/incorrect responses and reaction times associated with correct responses. We link the hidden performance state to the MPP observation, which accounts for the reaction times merely when the correct response occurs. We use the particle filtering within the EM algorithm to decode the hidden state. In particular, we design a particle filter that enables us to handle the non-linearity induced by the ARCH process noise. To evaluate the designed decoder, we use the simulated data as well as experimental data recorded during the n-back task in the presence of music stimuli.

II. METHODS

A. Data

In this research, we employ a publicly available dataset, which incorporates the n-back experiments in the presence of safe interventions such as music [31]. The studied n-back experiment was initially presented in [2]. The experimental procedures were approved by the IRB at the University of Houston, TX, USA (STUDY 00002490). A total number of 17 subjects took part in the experiment, with 7 subjects were excluded from the original study due to measurement errors and artifacts, and 10 subjects were studied (Subject A1-A10). The consent forms were obtained from all of the subjects prior to the experiment. During the n-back task, a series of stimuli (e.g., English alphabet) were presented to the subject, and the subject was required to verify if the current stimulus matched the n^{th} previous one. The 1-back and 3-back task blocks were equally and randomly distributed across 4 sessions: No background music was played in the first session; the relaxing and exciting background music were included in the second and third sessions, respectively; the fourth session contrived with a newly generated relaxing music via deep learning neural networks [2]. A total number of 16 task blocks were implemented at each session. Each task block included 5 seconds of instruction followed by 22 trials. Each trial included 0.5 seconds of stimulus display followed by 1.5 seconds plus sign. The 10-second resting time was provided at the end of each task block. Also, there were 20-second resting periods in the middle of each session. In total, a subject performed 1408 trials (i.e., 4 sessions x 16 task blocks \times 22 trials). A detailed description of the experiment is presented in [2].

B. State-space Model

Inspired by the proposed performance state model in [7], [8], we consider the following AR(1)-ARCH(1) model for the hidden performance state (z_j) :

$$z_j = z_{j-1} + \epsilon_j, \tag{1}$$

where the process noise term ϵ_j follows the ARCH structure, and $\epsilon_j \sim \mathcal{N}(0,h_j^2)$ such that the process noise variance h_j^2 varies over the time, and can be written as $h_j^2 = \alpha_0 + \alpha_1 \epsilon_{j-1}^2$. The terms α_0 and α_1 are the unknown ARCH model parameters to be determined.

To decode the hidden performance state, an observation vector needs to be specified. Here, we form the observation vector Y^j from the sequence of responses n_j as well as the log of reaction time $log(t_j)$. The observation can be written in the MPP form such that the continuous log of reaction time (i.e., $r_j = log(t_j)$) stands for the marked, and the correct response denotes the observed point process (i.e., $n_j = 1$). We indicate the correct response indices by $\tilde{J} = \{j | n_j = 1\}$.

The sequence of responses is assumed to be a Bernoulli-distributed random variable with probability mass function $p_j^{n_j}(1-p_j)^{1-n_j}$; the probability of having a correct response $p_j = P(n_j = 1)$ can be related to performance state using the logit transformation [7], [10], [30]:

$$p_j = \frac{1}{1 + e^{-(\mu + z_j)}}. (2)$$

The constant term μ can be determined from $\mu \approx \log\left(\frac{\bar{p}}{1-\bar{p}}\right)$ where \bar{p} is the average probability of observing a correct response (i.e., $\bar{p} = \frac{\sum_{j=1}^{j=J} n}{J}$) [7], [10], [18], [32].

Also, the marked observation can be linked to the hidden state using the following linear function [18]:

$$r_{j\in\tilde{J}} = \gamma_0 + \gamma_1 z_j + v_j,\tag{3}$$

where $r_j = log(t_j)$ is considered merely in the presence of the correct responses (i.e., $j \in \tilde{J}$); the term $v_j \sim \mathcal{N}(0, \sigma_v^2)$ stands for the measurement noise, and γ_0 and γ_1 are the unknown parameters to be recovered.

Therefore, the joint density function can be written as

$$p(n_j \cap r_j | z_j) = \begin{cases} 1 - p_j & \text{if } n_j = 0\\ p_j \frac{1}{\sqrt{2\pi\sigma_v^2}} e^{\frac{-(r_j - \gamma_0 - \gamma_1 z_j)^2}{2\sigma_v^2}} & \text{if } n_j = 1 \end{cases}$$
(4)

To decode the hidden performance state and recover the unknown model parameters at the same time, the EM algorithm can be employed [7], [18].

C. State-space Decoder

To simultaneously decode the state and recover the unknown model parameters $\theta_p = \{\gamma_0, \gamma_1, \sigma_v^2, \alpha_0, \alpha_1\}$ from the observation vector $Y^J = \{(n_1, r_1), (n_2, r_2), ..., (n_J, r_{J \in \tilde{J}})\}$, the EM algorithm can be utilized. However, including the ARCH noise within the state model introduces non-linearity [33]. To handle the non-linearity, we use a particle filtering approach [7], [8], [33]. We decode the hidden performance at the E-step, and recover the model parameters θ_p at the M-step [7], [8], [33]. Inspired by the presented framework in [7] and [33], we design a decoder that enables us to decode the performance from the MPP-type observation. The E-step and M-step derivations are shown below:

E-Step:

- Step 1: Generate K number of particles by setting the initial process noise variance to its unconditional and stationarity value (i.e., $h_0^2 = \frac{\alpha_0}{1-\alpha_1}$), and assuming an arbitrary initial mean state value \bar{z}_0 and state variance σ_0^2 .
- Step 2: Move forward from j-1 to j and generate particles $\hat{z}_j(k)$ based on the proposed distribution π such that $\hat{z}_j(k) \sim \mathcal{N}\left(\bar{z}_j(k), \sigma_j^2(k)\right)$ where \bar{z}_j stands for conditional state mean, and σ_j^2 denotes the conditional variance [7].

Case when n=0:

$$\bar{z}_{j}(k) = \left(\sigma_{j-1}^{2}(k) + h_{j}^{2}(k)\right) \left(n_{j} - \bar{p}_{j}(k)\right) + \hat{z}_{j-1}(k),$$

$$\sigma_{j}^{2}(k) = \left[\frac{1}{\sigma_{j-1}^{2}(k) + h_{j}^{2}(k)} + \bar{p}_{j}(k)\left(1 - \bar{p}_{j}(k)\right)\right]^{-1}$$
(6)

Case when n=1:

$$\bar{z}_{j}(k) = \frac{\sigma_{j-1}^{2}(k) + h_{j}^{2}(k)}{\gamma_{1}^{2} \left(\sigma_{j-1}^{2}(k) + h_{j}^{2}(k)\right) + \sigma_{v}^{2}} \left[\sigma_{v}^{2} \left(n_{j} - \bar{p}_{j}(k)\right) + \gamma_{1} \left(r_{j} - \gamma_{0} - \gamma_{1}\hat{z}_{j-1}(k)\right) + \hat{z}_{j-1}(k), \right] + \gamma_{1} \left(r_{j} - \gamma_{0} - \gamma_{1}\hat{z}_{j-1}(k)\right) + \hat{z}_{j-1}(k),$$

$$\sigma_{j}^{2}(k) = \left[\frac{1}{\sigma_{j-1}^{2}(k) + h_{j}^{2}(k)} + \bar{p}_{j}(k) \left(1 - \bar{p}_{j}(k)\right) \right]$$

$$+ \frac{\gamma_{1}^{2}}{\sigma_{v}^{2}} \right]^{-1}$$

$$+ \frac{\gamma_{1}^{2}}{\sigma_{v}^{2}}$$
(8)

where $h_i^2(k)$ can be derived from

$$h_j^2(k) = \alpha_0 + \alpha_1 \left(\hat{z}_{j-1}(k) - \hat{z}_{j-2}(k)\right)^2.$$
 (9)

By plugging $\bar{p}_j(k) = \left[1 + e^{-(\mu + \bar{z}_j(k))}\right]^{-1}$ in (5) as well as (7), the term $\bar{z}_j(k)$ would appear on both sides,

- and one can solve for $\bar{z}_j(k)$ by incorporating numerical approaches such as Newton Raphson.
- Step 3: Specify the importance weight $w_j(k)$ of each sample $\hat{z}_j(k)$ using the weight density function of interest. Here, given the proposed distribution π , we employ the sequential importance sampling (SIS) [34], [35], and the importance weight w_j can be obtained from

$$w_{j}^{(k)} = w_{j}^{(k-1)} \frac{p\bigg(n_{j} \cap r_{j} | \hat{z}_{j}(k)\bigg) p\bigg(\hat{z}_{j}(k) | \hat{z}_{j-1}(k)\bigg)}{\pi\bigg(\hat{z}_{j}(k) | \hat{z}_{0:j-1}(k), Y^{0:j}\bigg)}.$$
(10)

- Step 4: To avoid the particle degeneracy, normalize the weights $w^{(k)}{}_j = \frac{w^{(k)}_j}{\Sigma w^{(1:K)}_j}$ and execute particle resampling [7], [36]. Following the proposed approach in [37], the effective sample size can be approximated as $N_{ess} = \frac{1}{\Sigma_{k=1:K} w^2_j(k)}$. Assigning K/2 as the threshold, if $N_{ess} < K/2$, the residual resampling can be executed [38], [39].
- Step 5: After proceeding in the forward direction (j = J), we reverse the direction and derive a set of smoothed state $\tilde{z}_j(k)$ with equally smoothed weights $\tilde{w}_j(k) = 1/K$ from the distribution of interest. To mitigate the risk of overfitting, we consider $p(\tilde{z}_j(k-1)|\hat{z}_j(k))$ as the distribution of interest and evolve the smoothed state solely based on the dynamics of the system. [7], [40].

M-Step: At the M-step, the unknown model parameters can be recovered such that they maximize the expected value of log-likelihood function. The expected value of the log-likelihood $\mathbb{E}[Q(z_j,\theta_p)]$ can be approximated as $\mathbb{E}[Q(z_j,\theta_p)] \approx \frac{1}{K} \sum_{k=1}^K Q\Big(\tilde{z}_j(k),\theta_p\Big)$, where the log-likelihood function (Q) is presented as [7], [8], [33], [41]:

$$Q = \sum_{j=1}^{J} \left[n_{j} (\beta + z_{j}) - \log(1 + e^{\beta + z_{j}}) \right]$$

$$+ \frac{-|\tilde{J}|}{2} \log(2\pi\sigma_{v}^{2}) - \sum_{j \in \tilde{J}} \frac{(r_{j} - \gamma_{0} - \gamma_{1}z_{j})^{2}}{2\sigma_{v}^{2}}$$

$$+ \frac{-J}{2} \log(2\pi) - \frac{1}{2} \sum_{j=1}^{J} \left[\frac{(z_{j} - z_{j-1})^{2}}{\alpha_{0} + \alpha_{1}(z_{j-1} - z_{j-2})^{2}} + \log\left(\alpha_{0} + \alpha_{1}(z_{j-1} - z_{j-2})^{2}\right) \right].$$

$$(11)$$

The term J denotes the indices of correct responses. Hence, we may find a set of parameters $\theta_p = \{\gamma_0, \gamma_1, \sigma_v^2, \hat{\alpha}_0, \hat{\alpha}_1\}$ that maximizes the $\mathbb{E}[Q(z_j, \theta_p)]$ [7], [8]. The algorithm iterates between the E-step and the M-step until convergence.

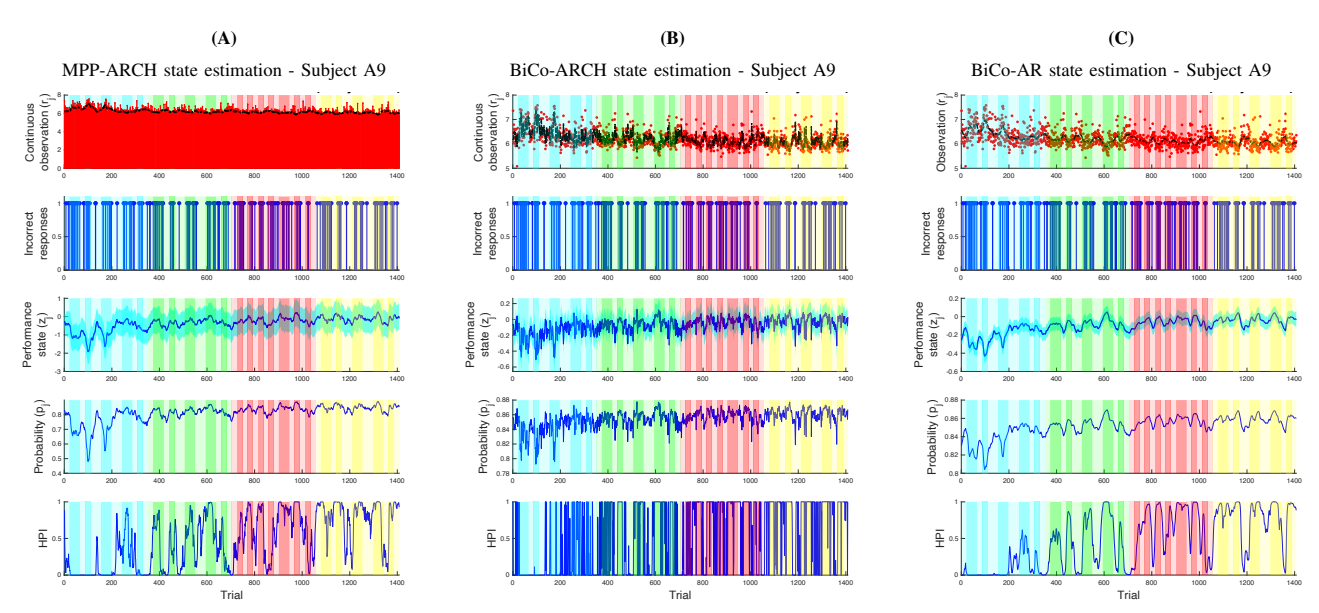


Fig. 1: The decoded cognitive performance state using experimental data. The sub-figures from left to right present: (A) the MPP-ARCH decoder findings, (B) the BiCo-ARCH decoder findings [8], and (C) the BiCo-AR decoder findings on experimental data [2], [8]. In each sub-figure, the sub-panels, in turn, depict: The applied observation (red) and its fit (black); the sequence of incorrect responses (blue vertical line); decoded performance state (blue) and its 95% confidence limits; the decoded probability (blue); the HPI (blue). The cyan, green, red, and yellow background colors correspond to the no music, relaxing, exciting, and generated relaxing music sessions, respectively.

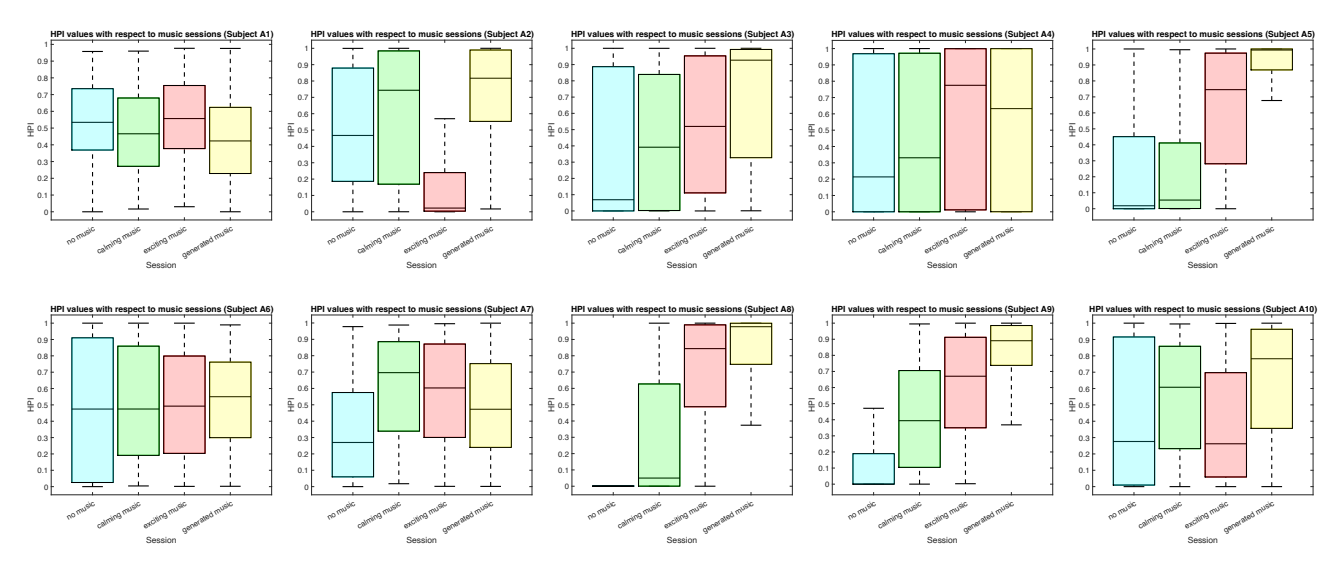


Fig. 2: Distribution of HPI within different music sessions derived from MPP-ARCH decoder. Each sub-figure presents the box plots of HPI with respect to music sessions for each subject. Each box shows the HPI within the music session of interest. The cyan, green, red, and yellow background colors correspond to the no music, relaxing, exciting, and generated relaxing music sessions, respectively.

III. RESULTS

We test the designed decoder on both the experimental and simulated data. In particular, we use the music intervention dataset in [2], and apply the existing BiCo-based decoders (i.e., BiCo-AR and BiCo-ARCH) as well as MPP-ARCH decoder. To simulate a set of data, we set the model parameters similar to [7], [8].

The performance state estimations based on experimental data are depicted in Fig. [I] From left to right, sub-figures present: (A) The estimated performance based on the developed MPP-ARCH decoder; (B) The estimated performance from BiCo-ARCH decoder developed in [7]; (C) The

estimated performance associated with BiCo-AR decoder [2], [9], [10], [30]. Within each sub-figure, the subplots, from top to bottom, show the applied observation r_j (red) and the fitted (i.e., reconstructed) one (black), a sequence of incorrect responses, estimated performance state (blue), estimated probability (blue), and the high performance index (HPI). It should be noted that while the developed MPP-ARCH decoder here uses MPP observation (i.e., $r_{j \in \bar{J}}$), the previously applied BiCo-based decoders employ pairs of binary and continuous observations (i.e., r_{j} is observed at each time index).

In regard to the experimental data, the absence of ground

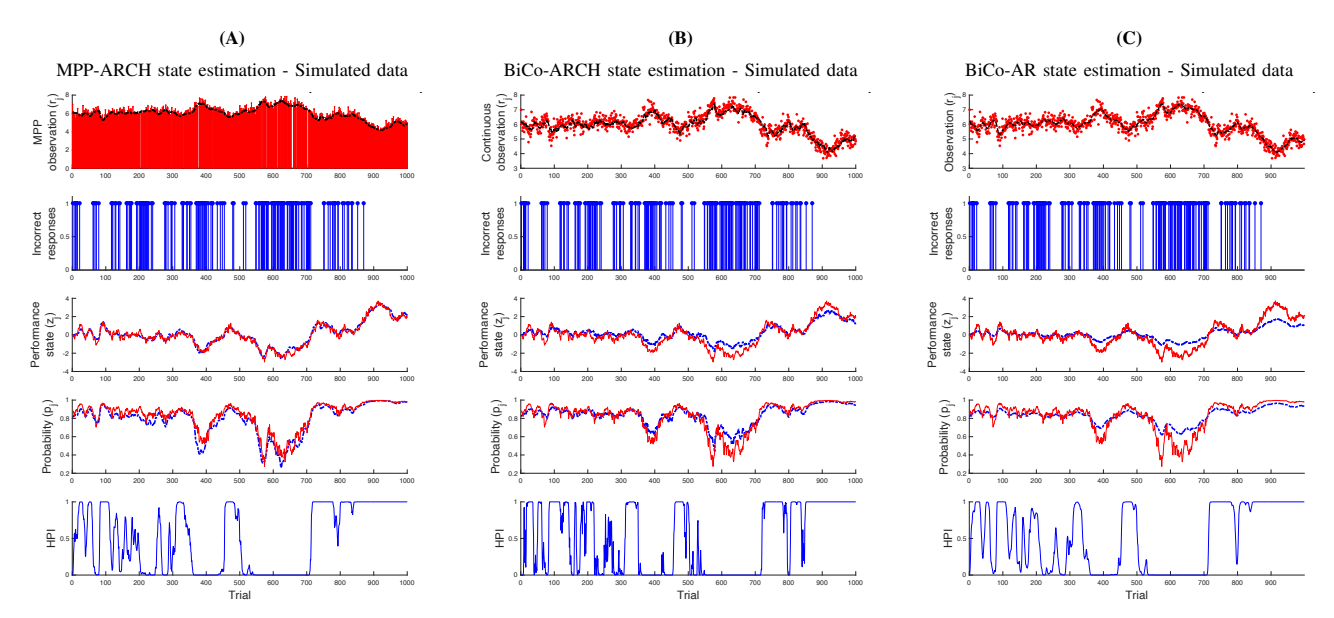


Fig. 3: The decoded cognitive performance state using simulated data. The sub-figures from left to right present: (A) the MPP-ARCH decoder findings, (B) the BiCo-ARCH decoder findings, and (C) the BiCo-AR decoder findings on simulated data. In each sub-figure, the sub-panels, in turn, depict: The applied observation (red) and its fit (black); the sequence of simulated incorrect responses (blue vertical line); the simulated performance state (red) and the decoded performance state (blue); the simulated probability (red) and the decoded probability (blue); the HPI (blue).

truth may lead to an implicit evaluation of the decoder. As an instance of such implicit evaluation, we fit (i.e., reconstruct) the employed MPP observation by plugging the decoded state into $\gamma_0 + \gamma_1 z_j$, and we evaluate if the reconstructed signal can capture the trend. To further assess the performance of the decoder, we can focus on the cluster of incorrect responses and expect to observe a decrease in the estimated performance.

In order to have a general and person-specific index of performance, we formulate the HPI, derived from the $p(z_j > z_{\rm threshold})$, where the threshold is set to be the median of the subject's performance state [1], [8]. This type of index is between zero and one, and it is known as the ideal observer certainty level [18]. In the context of behavioral learning, HPI mainly presents the probability that a correct response occurs more than just by chance [18], [19]. We depict the box plot of HPI with respect to each music session for all subjects in Fig. [2]

The sub-figures of Fig. 3 depict the estimated performance associated with the simulated data using the MPP-ARCH decoder, BiCo-ARCH decoder, and BiCo-AR decoder, respectively. The subplots, from top to bottom, present the applied observation r_j (red) and the fitted one (black), the simulated sequence of incorrect response, the simulated performance state (red) and estimated one (blue), the simulated probability (red) and estimated one (blue), and the HPI. The mean squared error (MSE) of estimated performance state associated with the MPP-ARCH decoder, BiCo-ARCH decoder, and BiCo-AR decoder are 0.0807, 0.2969, and 0.5207, respectively.

IV. DISCUSSION

Given the findings on the experimental data and comparing the estimated HPI in depicted decoders (Fig. []), we can

note the instances of performance overestimation: Comparing MPP-ARCH and BiCo-AR decoders, at trials 600-622, where a relatively high number of incorrect responses are gathered, the HPI derived from the BiCo-AR decoder is constantly high while this is not the case for the estimated HPI via the MPP-ARCH decoder. Also, an example of performance underestimation can be noted in the BiCo-AR decoder, where the estimated HPI during the end of calming session is persistently low regardless of the observed correct responses. On the other hand, the decoded performance from the BiCo-ARCH decoder tends to overfit to the continuous reaction time.

Looking into the decoded HPI via MPP-ARCH decoder in Fig. 2, and considering subjects A2 and A10, the median of HPI is higher in both of the relaxing sessions compared to no music and exciting music sessions. It should be noted that the median of HPI in the music session with generated relaxing music is slightly higher than in the session with the subject provided relaxing music. The lowest HPI values are associated with the exciting session. The median HPI for no music session (i.e., control group) falls between the exciting and both relaxing sessions. Conversely, subjects A1 and A4 have a higher HPI during the exciting session compared to relaxing sessions. Subject A7 displays a higher HPI during the first relaxing session with the provided music, while we have a reduced HPI in the last session with the generated music. On the other hand, four subjects presented higher HPI during the exciting session compared to the relaxing session with the provided music, while the highest median of HPI occurred during the generated music session (subjects A3, A5, A8, and A9). It should be noted that the only subject that does not present considerable HPI difference (with respect to median of HPI) across the music sessions is subject A6.

It is worth highlighting that we can observe multiple trends

among the subjects, which can be an indicator of the personspecific nature of the cognitive function and brain structure [1]. Following the Yerkes-Dodson law from psychology [1], [42], [43], which suggests that a moderate level of arousal –another hidden cognitive state– can result in optimal performance, one may assume that the baseline of arousal state in subjects A2 and A10 is high, and exciting music may arouse the subjects such that the subjects surpass the optimal arousal level [1]. On the other hand, in subjects A2 and A10, the level of arousal baseline might be very low during the relaxing sessions, and exciting music helps the subjects to become aroused enough to have a better performance in the exciting session. However, future investigations in which the arousal will be decoded in a similar adaptive manner are needed to evaluate these assumptions. Additionally, to draw a high-resolution conclusion about the music's impact on performance, potential confounding factors such as fatigue level and habituation or learning effect need to be evaluated carefully [1]. We may note that this study is primarily dedicated to the performance decoder design procedures.

Findings on experimental data and the MPP-ARCH decoder outcome reveal an agreement between the applied observation and the estimated state. In particular, the values of the decoded state and probability decrease aligned with the cluster of incorrect responses. Also, the decoded HPI values vary with respect to the type of music. The ARCH process may preserve the environmental impact in the performance state dynamics. Here, we consider the music as the environmental factor that might interact with performance. It should be noted that the presented decoder has a relatively high degree of freedom, which can potentially cause overfitting. To address this concern, an overfitting control technique can be employed [32]. Another point to note is the complexity of the applied particle filter, which may result in a high computational cost.

In regard to the simulation study (Fig. 3), the MPP-ARCH decoder seems to provide a relatively reliable estimate given the MSE values, and it outperforms the BiCo-ARCH and BiCo-AR decoders. It can be seen that the adaptivity of the ARCH-based decoders enables decoding the tiny variation in performance state, whereas the decoded performance based on the BiCo-AR decoder does not capture the existing variations associated with the ground truth (i.e., simulated performance state).

V. CONCLUSION AND FUTURE WORK

In this research, we design a performance state decoder that accounts for the non-linearity of the process noise of the performance state dynamic as well as its volatile nature. Particularly, we enable the performance state model to preserve the volatility within the ARCH process noise. To avoid potential overestimation of performance, we consider the MPP-type observation, and we filter out the continuous reaction times associated with the incorrect responses. In general, the proposed decoder is able to reliably decode the hidden performance state from the MPP-type observation in

the presence of time-varying process noise variance. Specifically, the use of particle filtering within the EM algorithm enables simultaneous state and parameter estimation.

In the future, we aim to employ and evaluate the decoder in different experimental settings. Specifically, the decoder can be applied to various behavioral experiments with a wide range of interventions, such as auditory, gustatory, visual, and olfactory stimulation [2]. Another point to be considered is that in this study, we narrow down our attention to one basic cognitive function by focusing on the n-back task. The proposed framework can be further applied to decode the cognitive performance in various tasks, in which they utilize basic and higher-level cognitive functions at the same time.

Furthermore, we plan to study the reaction time and cognitive arousal link to investigate the feasibility of using reaction time as a common behavioral observation to decode arousal and performance concurrently [44]. Also, since the n-back task can be a repetitive task [10], identifying the link between the state of cognitive arousal and performance can pave the way for a new avenue of intervention design procedures.

REFERENCES

- [1] S. Khazaei, M. R. Amin, M. Tahir, and R. T. Faghih, "Bayesian inference of hidden cognitive performance and arousal states in presence of music," *IEEE Open Journal of Engineering in Medicine and Biology*, 2024.
- [2] H. Fekri Azgomi, L. R. F. Branco, M. R. Amin, S. Khazaei, and R. T. Faghih, "Regulation of brain cognitive states through auditory, gustatory, and olfactory stimulation with wearable monitoring," *Scientific Reports*, vol. 13, no. 1, p. 12399, 2023.
- [3] R. F. Engle, "Autoregressive conditional heteroscedasticity with estimates of the variance of united kingdom inflation," *Econometrica: Journal of the econometric society*, pp. 987–1007, 1982.
- [4] L. Tao, K. E. Weber, K. Arai, and U. T. Eden, "A common goodness-of-fit framework for neural population models using marked point process time-rescaling," *Journal of computational neuroscience*, vol. 45, pp. 147–162, 2018.
- [5] X. Deng, D. F. Liu, K. Kay, L. M. Frank, and U. T. Eden, "Clusterless decoding of position from multiunit activity using a marked point process filter," *Neural computation*, vol. 27, no. 7, pp. 1438–1460, 2015.
- [6] M. C. Burkhart, A discriminative approach to Bayesian filtering with applications to human neural decoding. ProQuest Dissertations Publishing, 2019.
- [7] S. Khazaei, M. R. Amin, and R. T. Faghih, "Decoding a neurofeedback-modulated performance state in presence of a timevarying process noise variance," in 2022 56th Asilomar Conference on Signals, Systems, and Computers, pp. 990–996, IEEE, 2022.
- [8] S. Khazaei and R. T. Faghih, "Decoding a cognitive performance state from behavioral data in the presence of auditory stimuli," *IEEE Transactions on Neural Systems and Rehabilitation Engineering*, 2024.
- [9] S. Khazaei, M. R. Amin, and R. T. Faghih, "Decoding a neurofeedback-modulated cognitive arousal state to investigate performance regulation by the yerkes-dodson law," in 2021 43rd Annual International Conference of the IEEE Engineering in Medicine and Biology Society (EMBC), IEEE, 2021.
- [10] M. R. Amin, M. Tahir, and R. T. Faghih, "A state-space investigation of impact of music on cognitive performance during a working memory experiment," in 2021 43rd Annual International Conference of the IEEE Engineering in Medicine & Biology Society (EMBC), pp. 757– 762, IEEE, 2021.
- [11] A. D. Baddeley and G. Hitch, "Working memory," in *Psychology of learning and motivation*, vol. 8, pp. 47–89, Elsevier, 1974.
- [12] T.-Y. Hou and W.-P. Cai, "What emotion dimensions can affect working memory performance in healthy adults? a review," World Journal of Clinical Cases, vol. 10, no. 2, p. 401, 2022.

- [13] M. Schütze, D. de Souza Costa, J. J. de Paula, L. F. Malloy-Diniz, C. Malamut, M. Mamede, D. M. d. Miranda, M. Brammer, and M. A. Romano-Silva, "Use of machine learning to predict cognitive performance based on brain metabolism in neurofibromatosis type 1," *PLoS One*, vol. 13, no. 9, p. e0203520, 2018.
- [14] M. Stikic, R. R. Johnson, D. J. Levendowski, D. P. Popovic, R. E. Olmstead, and C. Berka, "Eeg-derived estimators of present and future cognitive performance," *Frontiers in human neuroscience*, vol. 5, p. 70, 2011.
- [15] O. G. Sani, H. Abbaspourazad, Y. T. Wong, B. Pesaran, and M. M. Shanechi, "Modeling behaviorally relevant neural dynamics enabled by preferential subspace identification," *Nature Neuroscience*, vol. 24, no. 1, pp. 140–149, 2021.
- [16] A. Yousefi, R. Kakooee, M. T. Beheshti, D. D. Dougherty, E. N. Eskandar, A. S. Widge, and U. T. Eden, "Predicting learning dynamics in multiple-choice decision-making tasks using a variational bayes technique," in 2017 39th Annual International Conference of the IEEE Engineering in Medicine and Biology Society (EMBC), pp. 3194–3197, IEEE, 2017.
- [17] A. Yousefi, A. C. Paulk, T. Deckersbach, D. D. Dougherty, E. N. Eskandar, A. S. Widge, and U. T. Eden, "Cognitive state prediction using an em algorithm applied to gamma distributed data," in 2015 37th Annual International Conference of the IEEE Engineering in Medicine and Biology Society (EMBC), pp. 7819–7824, IEEE, 2015.
- [18] D. S. Wickramasuriya and R. T. Faghih, "A marked point process filtering approach for tracking sympathetic arousal from skin conductance," *IEEE Access*, vol. 8, pp. 68499–68513, 2020.
- [19] A. C. Smith, L. M. Frank, S. Wirth, M. Yanike, D. Hu, Y. Kubota, A. M. Graybiel, W. A. Suzuki, and E. N. Brown, "Dynamic analysis of learning in behavioral experiments," *Journal of Neuroscience*, vol. 24, no. 2, pp. 447–461, 2004.
- [20] D. S. Wickramasuriya and R. T. Faghih, "A bayesian filtering approach for tracking arousal from binary and continuous skin conductance features," *IEEE Transactions on Biomedical Engineering*, vol. 67, no. 6, pp. 1749–1760, 2019.
- [21] D. S. Wickramasuriya and R. T. Faghih, "A cortisol-based energy decoder for investigation of fatigue in hypercortisolism," in 2019 41st Annual International Conference of the IEEE Engineering in Medicine and Biology Society (EMBC), pp. 11–14, IEEE, 2019.
- [22] D. S. Wickramasuriya and R. T. Faghih, "A mixed filter algorithm for sympathetic arousal tracking from skin conductance and heart rate measurements in pavlovian fear conditioning," *PloS one*, vol. 15, no. 4, p. e0231659, 2020.
- [23] D. S. Wickramasuriya, M. Amin, and R. T. Faghih, "Skin conductance as a viable alternative for closing the deep brain stimulation loop in neuropsychiatric disorders," *Frontiers in neuroscience*, vol. 13, p. 780, 2010
- [24] L. Bauwens, C. M. Hafner, and S. Laurent, Handbook of volatility models and their applications, vol. 3. John Wiley & Sons, 2012.
- [25] D. Ardia, Financial Risk Management with Bayesian Estimation of GARCH Models Theory and Applications. Springer, 2008.
- [26] B. K. Hawes, T. T. Brunyé, C. R. Mahoney, J. M. Sullivan, and C. D. Aall, "Effects of four workplace lighting technologies on perception, cognition and affective state," *International Journal of Industrial Ergonomics*, vol. 42, no. 1, pp. 122–128, 2012.
- [27] C. Kirschbaum, O. T. Wolf, M. May, W. Wippich, and D. H. Hell-hammer, "Stress-and treatment-induced elevations of cortisol levels associated with impaired declarative memory in healthy adults," *Life sciences*, vol. 58, no. 17, pp. 1475–1483, 1996.
- [28] H. Peak and E. G. Boring, "The factor of speed in intelligence.," Journal of Experimental Psychology, vol. 9, no. 2, p. 71, 1926.
- [29] I. J. Deary, G. Der, and G. Ford, "Reaction times and intelligence differences: A population-based cohort study," *Intelligence*, vol. 29, no. 5, pp. 389–399, 2001.
- [30] M. J. Prerau, A. C. Smith, U. T. Eden, Y. Kubota, M. Yanike, W. Suzuki, A. M. Graybiel, and E. N. Brown, "Characterizing learning by simultaneous analysis of continuous and binary measures of performance," *Journal of neurophysiology*, vol. 102, no. 5, pp. 3060–3072, 2009.
- [31] H. Fekri Azgomi, et al, "Regulation of brain cognitive states through auditory, gustatory, and olfactory stimulation with wearable monitoring." PhysioNet, doi: 10.13026/jr6f-wc85., Dec. 2023.
- [32] D. S. Wickramasuriya, S. Khazaei, R. Kiani, and R. T. Faghih, "A bayesian filtering approach for tracking sympathetic arousal and

- cortisol-related energy from marked point process and continuous-valued observations," *IEEE Access*, pp. 1–1, 2023.
- [33] J.-C. Duan and A. Fulop, "A stable estimator of the information matrix under em for dependent data," *Statistics and Computing*, vol. 21, no. 1, pp. 83–91, 2011.
- [34] A. Doucet, S. J. Godsill, and C. Andrieu, On sequential simulationbased methods for Bayesian filtering. Department of Engineering, University of Cambridge Cambridge, UK, 1998.
- [35] N. Vaswani, "Importance sampling and particle filtering,"
- [36] A. R. Poyatos-Bakker, V. Isanbaev-Sobolyev, J.-L. Blanco-Claraco, E. Viciana, J. Ventura, F. M. Arrabal-Campos, R. Baños, A. Alcayde, and F. G. Montoya, "Load disaggregation through particle filtering of harmonic features," in 2022 20th International Conference on Harmonics & Quality of Power (ICHQP), pp. 1–6, IEEE, 2022.
- [37] J. Elfring, E. Torta, and R. van de Molengraft, "Particle filters: A hands-on tutorial," Sensors, vol. 21, no. 2, p. 438, 2021.
- [38] A. Doucet, A. M. Johansen, et al., "A tutorial on particle filtering and smoothing: Fifteen years later," *Handbook of nonlinear filtering*, vol. 12, no. 656-704, p. 3, 2009.
- [39] J.-L. Blanco, "Resampling methods for particle filtering." https://www.mathworks.com/matlabcentral/fileexchange/24968-resampling-methods-for-particle-filtering, 2023.
- [40] A. Doucet, N. De Freitas, N. J. Gordon, et al., Sequential Monte Carlo methods in practice, vol. 1. Springer, 2001.
- [41] J. F. de Freitas, M. Niranjan, A. H. Gee, and A. Doucet, "Sequential monte carlo methods to train neural network models," *Neural computation*, vol. 12, no. 4, pp. 955–993, 2000.
- [42] R. M. Yerkes, *The dancing mouse*, vol. 1. Macmillan Company, 1907.
- [43] R. M. Yerkes, J. D. Dodson, *et al.*, "The relation of strength of stimulus to rapidity of habit-formation," 1908.
- [44] S. Alam, S. Khazaei, and R. T. Faghih, "Unveiling productivity: The interplay of cognitive arousal and expressive typing in remote work," *Plos one*, vol. 19, no. 5, p. e0300786, 2024.